

Polarization characteristics of nonlinear refraction and nonlinear scattering in several solvents

Xiao-Qing Yan,^{1,2} Zhi-Bo Liu,^{1,3} Yong-Sheng Chen,² and Jian-Guo Tian^{1,4}

¹The Key Laboratory of Weak Light Nonlinear Photonics, Ministry of Education, Teda Applied Physics School and School of Physics, Nankai University, Tianjin 300457, China

²The Key Laboratory of Functional Polymer Materials and Center for Nanoscale Science & Technology, Institute of Polymer Chemistry, College of Chemistry, Nankai University, Tianjin 300071, China

³e-mail: rainingstar@nankai.edu.cn

⁴e-mail: jjtian@nankai.edu.cn

Received May 22, 2012; revised July 21, 2012; accepted August 6, 2012;
posted August 13, 2012 (Doc. ID 169007); published September 11, 2012

The polarization characteristics of nonlinear refraction and nonlinear scattering in several solvents (toluene, o-dichlorobenzene, N, N-dimethylformamide) are studied using the polarized light Z-scan technique with femtosecond laser pulses. For nonlinear refraction, the physical mechanism of the polarization characteristics is that the nonlinear polarization component related to $\text{Re}(\chi_{xyyx}^{(3)})$ could be adjusted by polarization state of incident light in isotropic media. For nonlinear scattering, the polarization characteristic is related to the self-focusing effect, which depends on the nonlinear refractive index and polarization state of incident light. In addition, the values of nonlinear refractive indices and third-order nonlinear susceptibility components are determined for these solvents at the femtosecond time scale. Both nonresonant electronic nonlinearity and fast noninstantaneous nuclear nonlinearity contribute to these values at the pulse width used in the measurements. Also, these nonlinear refractive indices and third-order nonlinear susceptibility components could be used in calculating nonlinear optical parameters of those novel materials that need to be dissolved in these solvents in nonlinear optical measurements. © 2012 Optical Society of America

OCIS codes: 320.7110, 190.5890, 290.5855, 120.6710.

1. INTRODUCTION

In the past decades, the polarization characteristics of nonlinear optical properties have been reported in various materials [1]; these nonlinear optical properties include nonlinear refraction [2,3], nonlinear absorption [4–6], and nonlinear scattering [7,8]. In these polarization characteristics measurements, the linearly polarized light was usually used, and circularly polarized light was occasionally used. The materials studied are mostly like crystal, waveguide, optical fiber, and other solid materials [2–8]. The polarization characteristics of nonlinear optical properties in liquid solvents are rarely studied by using different polarized light (linearly, elliptically, and circularly).

As we know, the nonlinear refraction originates from the nonlinear polarization \mathbf{P} , which is related to the field amplitudes by the nonlinear susceptibility tensor [9,10]. In isotropic media, there are only two independent tensor elements among the 21 nonzero third-order susceptibility tensor elements when the field frequencies are degenerate, i.e., $\chi_{xyyy}^{(3)}$ and $\chi_{xyyx}^{(3)}$ [9,10]. The one component in nonlinear polarization \mathbf{P} is from the process related to $\chi_{xyyx}^{(3)}$, and the contribution in nonlinear polarization \mathbf{P} from this component could be adjusted by the polarization state of the incident beam [9,11–13]. Thus, the nonlinear refraction (NLR) of isotropic media depends on the polarization state of the incident beam [9,11–13]. Liquid solvent is a type of isotropic material with a high degree of spatial symmetry [9]. The NLR in solvent should be a function of polarization state of incident beam.

Self-focusing is a nonlinear optical process induced by positive NLR of materials exposed to intense electromagnetic radiation [9,14–16]. The peak intensity of the self-focused region could keep increasing as the wave travels through the medium, until defocusing effects or medium damage interrupt this process [15,16]. It is well known that the self-focusing effect changes with the polarization state in isotropic media because the nonlinear refractive index is a function of polarization state [i.e., the anisotropy of $\text{Re}(\chi_{xyyx}^{(3)})$ for different polarized light] [15–18]. Because of self-focusing effect, both the intensity distribution and the maximum intensity are functions of the polarization state during the light propagating in isotropic media. However, the nonlinear scattering (NLS) and laser-induced damage (LID) greatly relate to the light intensity as reported in [15,19–27]. So the NLS in isotropic media should be a function of polarization state too. At present, there is no experimental report on polarization dependence of NLS in solvents.

Toluene, o-dichlorobenzene (ODCB), and N, N-dimethylformamide (DMF) are liquid solvents. In nonlinearity measurements of novel materials, they are widely used as solvents [28–31]. At present, there are no reports on the polarization characteristics of their nonlinear optical properties. In order to extract accurately nonlinear susceptibility values of the novel materials (dissolved in these solvents) from the NLR signal of the solution, it is necessary to know these nonlinear susceptibility components values for these solvents at first. However, the reports on nonlinear susceptibility component values of these solvents are absent at present.

Here we studied the polarization characteristics of NLR and NLS in the three solvents by using a polarized light Z-scan method with femtosecond (fs) laser pulses ($\lambda = 800$ nm, $\tau_{\text{FWHM}} = 125$ fs). Furthermore, the third-order nonlinear susceptibility tensor elements are determined from the nonlinear refractive indices of linearly and circularly polarized light. The purposes of this article are both to experimentally present the polarization characteristic of NLR and NLS in these solvents and to provide the third-order nonlinear susceptibility tensor elements values for them.

2. EXPERIMENTAL ARRANGEMENT

The experimental setup was the same as the one in [13]. A Ti-sapphire mode-locked laser system (Spitfire Pro, Spectra Physics) providing 120 fs (FWHM) pulses was used for the light source. The repetition rate was 1 KHz, and the wavelength was 800 nm. The near-Gaussian spatial distribution was produced by a spatial filter placed before the setup. The spatial distribution of the incidence pulses was confirmed by a CCD camera (L230, LBA-USB-L230, Spiricon). The polarization state was changed by rotating a $\lambda/4$ wave plate, which was placed after a polarizer. The ellipticity of all the elliptically polarized light was set $e = \tan(5\pi/36)$ without special physical aim. We chose this ellipticity because the closed-aperture (CA) Z-scan trace at this polarization state could be easily distinguished from those of linearly and circularly polarized light. After the incident light passed the polarizer and wave plate, the pulse width had been broadened to be ~ 125 fs. The laser beam was focused by a 250 mm focal-length lens onto the sample. The beam waist radius of the focused laser beam was determined to be 30 ± 2 μm from a CCD camera (the pulse energy should be attenuated to an extremely low level at this time), and the beam waist radius was confirmed by the fitting quality of CA Z-scan traces shown below (i.e., comparison of $x_{T_{\text{peak}}-T_{\text{valley}}}$ between theoretical fit and experiment) [32]. The sample was the solvent held in a quartz cell. The reference and transmitted pulse energies were simultaneously measured by two detectors (Ophir). The measurement system was calibrated with ZnSe [open-aperture (OA) Z scan at low intensity] [33,34] and CS₂ (CA Z scan) [35–37], and calibration results of ZnSe and CS₂ are shown in Fig. 1. The two-photon absorption coefficient β of ZnSe and nonlinear refractive index of CS₂ are in good agreement with those reported in literature [our results, $\beta(\text{ZnSe}) = 2.5 \times 10^{-9}$ cm/W, $n_2(\text{CS}_2) = 3.0 \times 10^{-15}$ cm²/W]. It is noteworthy that our Z-scan experimental system is capable of resolving a normalized transmittance of $\sim 0.5\%$. These experiments were carried out at room temperature. Neither linear absorption nor linear scattering was observed in our measurements.

3. EXPERIMENTAL RESULTS AND DISCUSSION

A. NLR

In order to verify that the NLR is a function of the polarization state and obtain the values of $\text{Re}(\chi_{xyyy}^{(3)})$ and $\text{Re}(\chi_{xyyx}^{(3)})$, the polarized light CA Z-scan measurements were carried out at several field intensities for each solvent. In all the CA Z-scan measurements presented here, we had checked there was no NLS or nonlinear absorption at these input energies by carrying out OA Z-scan measurements at the same input energy. If there were NLS or nonlinear absorption at the input energy,

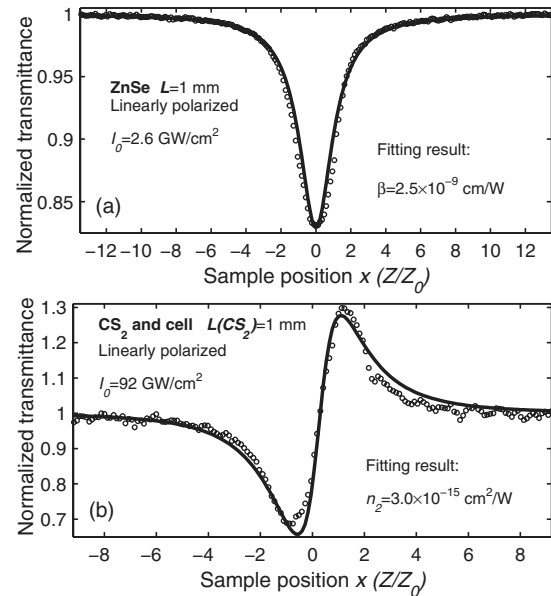


Fig. 1. (a) OA Z-scan trace of 1 mm ZnSe at 800 nm. (b) CA Z-scan trace of CS₂. The solid lines are theoretical fits, and fitting results are listed in the two figures.

there would be a dip at focus in the OA Z-scan trace. But we had not observed any dips in the corresponding OA Z-scan traces. In addition, when the sample was placed at focus, we had not observed any scattering signal from an infrared viewer at the input energy that is larger than the energy of CA Z-scan measurements but smaller than the energy used in the OA Z-scan measurements presented in the NLR section. We changed the sample for each Z-scan trace measurement (CA and OA) by laterally moving the sample in order to avoid LID of sample and false phenomenon in the measurements.

The linearly polarized light CA Z-scan trace of toluene (in cell) with on-axis peak intensity $I_0 = 380$ GW/cm² is shown in Fig. 2. Taking into account the NLR signal of the cell, the CA Z-scan measurement of the empty quartz cell was also conducted at each polarization state. As shown in Fig. 2, although the NLR signal of toluene in the cell is much larger than that of the empty cell, the NLR signal of the empty cell could not be ignored. The nonlinear refractive index $n_{2,\text{toluene and cell}} = 7.3 \times 10^{-16}$ cm²/W from theoretical fit is in good agreement with

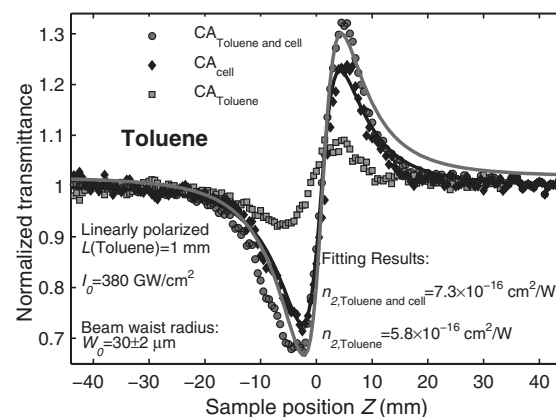


Fig. 2. Linearly polarized light CA Z-scan traces of toluene and cell, quartz cell, and toluene with $I_0 = 380$ GW/cm² and $L = 1$ mm.

others' work [$n_{2,\text{toluene and cell}} = (1.3 \pm 0.6) \times 10^{-19} \text{ m}^2/\text{W}$] [37]. To determine the contribution of the NLR signal of 1 mm thick toluene and the nonlinear refractive index $n_{2,\text{toluene}}$, the approximate NLR signal of 1 mm thick toluene was obtained by subtracting the NLR signal of the empty cell from that of "toluene and cell" ($T_{\text{solvent}} = 1 + T_{\text{solvent and cell}} - T_{\text{cell}}$). The approximate NLR index $n_{2,\text{toluene}}$ was obtained from a least-square fit of the theoretical equation to the CA Z-scan normalized transmittance T_{toluene} [10,11], and the $n_{2,\text{toluene}}$ is determined to be $5.8 \times 10^{-16} \text{ cm}^2/\text{W}$. From Fig. 2, we find that the theoretical curves fit the experimental data well. Because the NLR of the front cell wall changed slightly the spatial distribution of the incident beam in 1 mm thick toluene liquid, the obtained $n_{2,\text{toluene}}$ is not exactly true. At this intensity, the CA Z-scan measurements were also carried out by using circularly and elliptically polarized light, and the polarized light CA Z-scan measurements were carried out at another input energy.

The normalized transmittance curves of toluene (T_{toluene}) for different polarized light at $I_0 = 321 \text{ GW}/\text{cm}^2$ are shown in Fig. 3(a). There is some noise in these experimental data, especially for the circularly polarized light CA Z-scan trace. Clearly, the NLR signal decreases with ellipticity e . These polarized light CA Z-scan experimental data were analyzed using polarized light CA Z-scan theory [11]. The polarized light CA Z-scan theory could fit the experimental data well, and the nonlinear refractive index $n_{2,\text{toluene}}$ could be obtained from fitting [11]. As shown in Fig. 3(a), the nonlinear refractive index is largest for linearly polarized light ($n_{2,\text{lin}} = 5.6 \times 10^{-16} \text{ cm}^2/\text{W}$) and smallest for circularly polarized light ($n_{2,\text{cir}} = 3.3 \times 10^{-16} \text{ cm}^2/\text{W}$). For the linearly polarized light case, there is tiny deviation between experimental data and theoretical fit; the fitting result at this input energy is consistent with that at higher input energy as shown in Fig. 3(b). So these fitting results could be accepted although tiny deviation does exist.

Furthermore, the approximate values of the real part of the two susceptibility independent components can be calculated and listed in Fig. 3(a) [11]. The intensity and polarization dependence of $n_{2,\text{toluene}}$ is shown in Fig. 3(b). From the figure, we can find that $n_{2,\text{toluene}}$ decreases with ellipticity and keeps nearly constant for each polarization state in the measured intensity region, which means there is no higher-order NLR in our measurements. The solid lines are constant fitting results, and these fitting results are listed in Table 1. By combining the constant fitting results of linearly and circularly polarized light cases [9,11], the values of $\text{Re}(\chi_{xxxx}^{(3)})$, $\text{Re}(\chi_{yyyy}^{(3)})$, and $\text{Re}(\chi_{xyyx}^{(3)})$ could be determined as listed in Table 2.

The NLR of ODCB and DMF had been measured in the same way as toluene. The normalized transmittance curves T_{solvent} are shown in Figs. 4(a) and 5(a) for ODCB and DMF, respectively. By using a similar experimental data analysis method as toluene, the $n_{2,\text{solvent}}$ values could be obtained from fitting and are listed in the two figures. There is little deviation at the peak for the linearly polarized light CA Z-scan trace in ODCB as shown in Fig. 4(a). It may be from the tiny deviation of aperture center from the optical axis in the measurements. The deviation could not affect greatly the constant fitting results from Fig. 4(b). The intensity and polarization dependence of $n_{2,\text{solvent}}$ is shown in Figs. 4(b) and 5(b) for

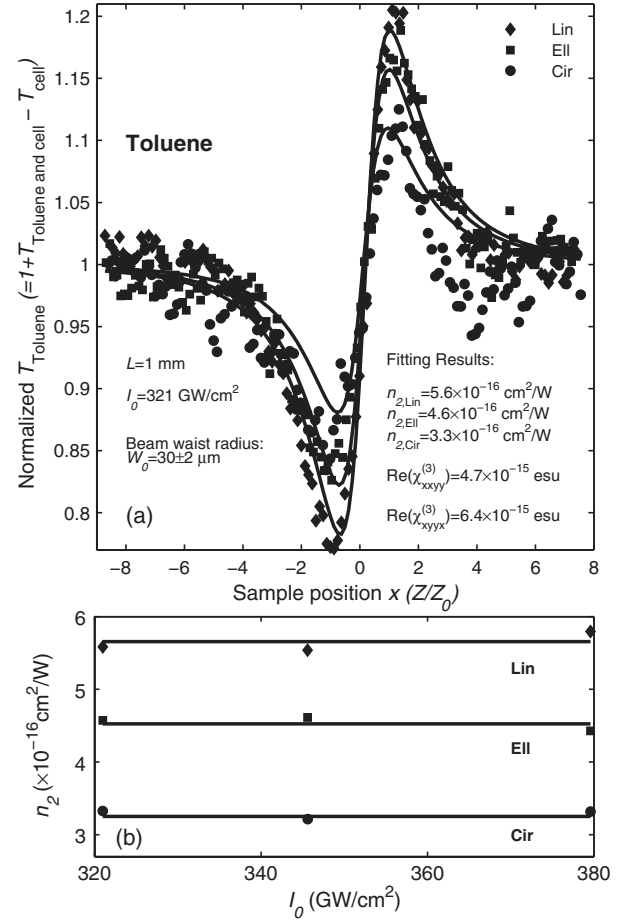


Fig. 3. (a) Normalized transmittance curve of toluene T_{toluene} for different polarized light at $I_0 = 321 \text{ GW}/\text{cm}^2$. (b) Dependence of nonlinear refractive index n_2 on I_0 and polarization state.

ODCB and DMF, respectively. From the dependence of nonlinear refractive index on intensity in ODCB and DMF, no higher-order nonlinearity in measurements could be concluded for the two solvents. The constant fitting results of $n_{2,\text{solvent}}$ for different polarized light are listed in Table 1. Furthermore, the third-order susceptibility component values of ODCB and DMF could be determined as listed in Table 2 in the same way as toluene.

From these polarized light CA Z-scan transmittance curves of the three solvents, the dependence of NLR on the polarization state of incident light in isotropic media is confirmed again. It is attributed to the ability to adjust the nonlinear polarization component related to $\text{Re}(\chi_{xyyx}^{(3)})$ by the polarization state of incident light in isotropic media. For the NLR originating from nonlinear polarization, the nonlinear

Table 1. Nonlinear Refractive Indices n_2 for Toluene, ODCB, and DMF with Different Polarized Light

	$n_2 (\times 10^{-16} \text{ cm}^2/\text{W})$		
	Linearly	Elliptically ($e = 0.4663$)	Circularly
Toluene	5.7	4.5	3.3
ODCB	4.8	3.7	2.8
DMF	4.0	3.0	2.2

Table 2. Values of Third-Order Nonlinear Susceptibility Components for Toluene, ODCB, and DMF

	Toluene	ODCB	DMF
$\text{Re}(\chi_{xxxx}^{(3)})$ ($\times 10^{-15}$ esu)	4.7	4.3	2.8
$\text{Re}(\chi_{xyyx}^{(3)})$ ($\times 10^{-15}$ esu)	6.6	6.0	4.8
$\text{Re}(\chi_{xxxx}^{(3)})$ ($\times 10^{-15}$ esu)	16.0	14.6	10.4
$\chi_{xyyx}^{(3)}/\chi_{xxxx}^{(3)}$	1.4	1.4	1.7

refractive index is a function of polarization state of incident beam [9,11].

For pure nonresonant electronic nonlinearity, $\chi_{xyyx}^{(3)}$ is equal to $\chi_{xxxx}^{(3)}$. The values of $\chi_{xyyx}^{(3)}/\chi_{xxxx}^{(3)}$ are larger than 1 for these solvents as listed in Table 2. There are both nonresonant electronic nonlinearity and fast noninstantaneous nuclear nonlinearity contributions to these nonlinear susceptibility components in our measurements at the fs time scale [38,39].

B. NLS

We used the OA Z -scan method to study qualitatively the polarization characteristics of NLS in these solvents [31]. During the measurements, we could observe the scattering signal by using an infrared viewer (FJW Optical Systems, Find-R-Scope) when the transmittance of sample at focus

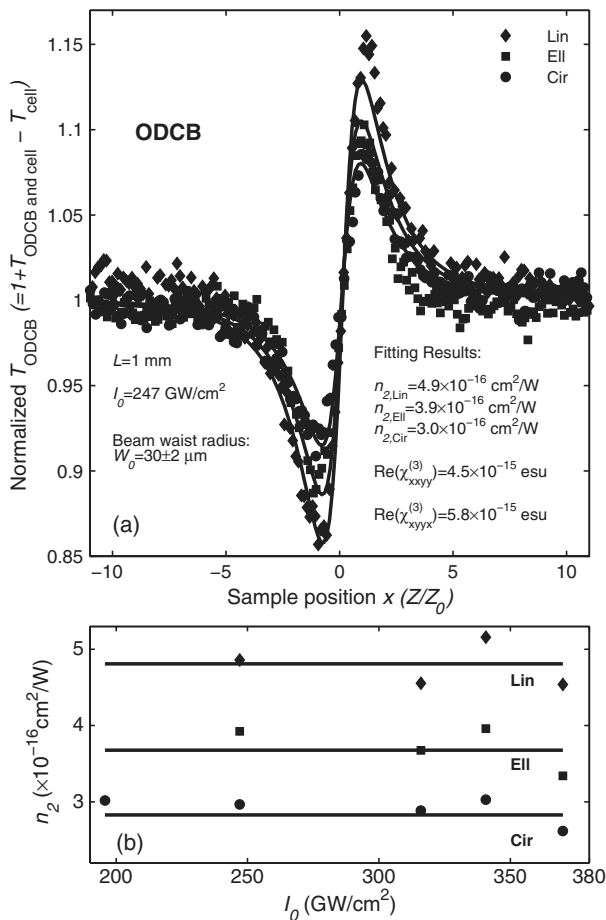


Fig. 4. (a) Normalized transmittance curve of ODCB T_{ODCB} for different polarization states at $I_0 = 247$ GW/cm². (b) Dependence of nonlinear refractive index n_2 on I_0 and polarization state.

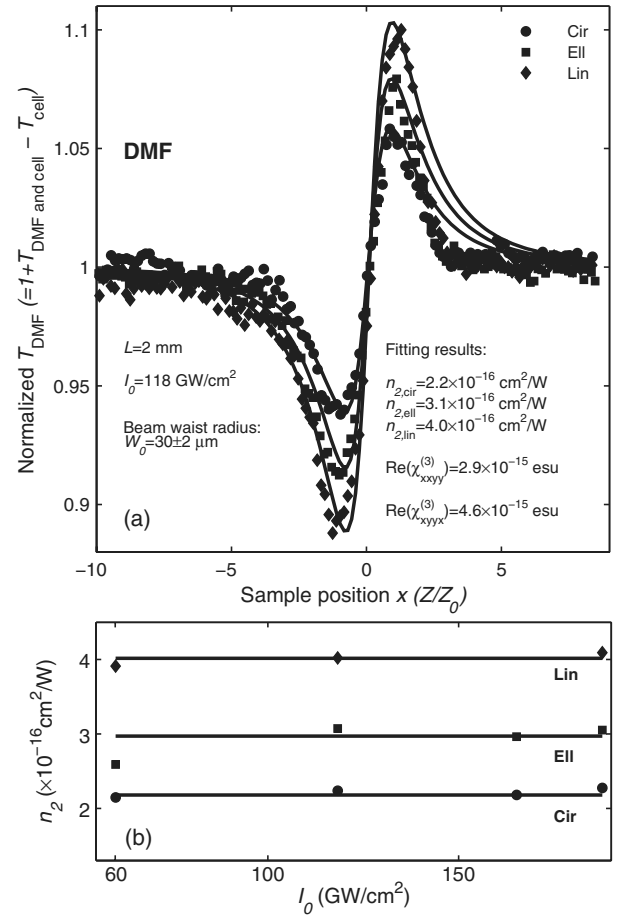


Fig. 5. (a) Normalized transmittance curve of DMF T_{DMF} for different polarized light at $I_0 = 118$ GW/cm². (b) Dependence of nonlinear refractive index n_2 on I_0 and polarization state.

decreased compared with that far away from focus. No nonlinear absorption signal in these OA Z -scan measurements had been confirmed.

Even at the largest pulse energy used in our measurements, we had not observed any signal of transmittance decreasing in the OA Z -scan trace of the empty quart cell (as shown in Fig. 11 below) or physical damage of the cell after these measurements. The NLS signal presented here should be from solvents. As reported in [27,40,41], the damage threshold of fused silica is larger than 6×10^{12} W/cm² at this range of pulse durations. The maximum intensity from simulation is below the damage threshold. So the signal from LID of the cell could be safely ruled out. From forward transmitted light spectra measurements (as shown in Fig. 6), the NLS was determined to be stimulated Rayleigh-wing scattering (SRWS) for ODCB and DMF. For toluene, there is stimulated Raman scattering besides the SRWS [9]. The observed SRWS in these solvents is similar to the observed scattering in CS₂ by using picosecond laser pulses [42].

The polarized light OA Z -scan traces of toluene for different sample lengths are shown in Fig. 7. From the figure, we find that the Z position Z_{decrease} where the normalized transmittance starts to decrease is getting away from focus when the ellipticity e decreases or the sample length L increases. Because of the decrease of normalized transmittance was from NLS, the position for NLS starting is getting away from

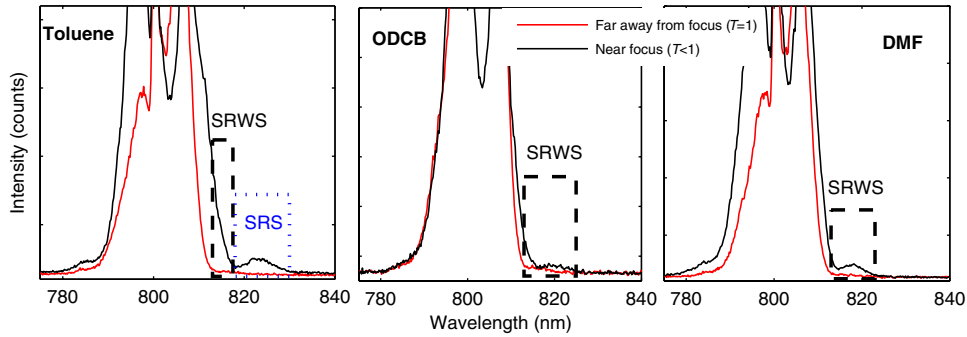


Fig. 6. (Color online) Comparison of forward transmitted light spectra at different sample position.

focus too. The NLS signal intensity increases with sample length and decreases with ellipticity e .

The polarization dependence of NLS could not originate from the intrinsic response of solvent molecule to polarized light. As shown in Fig. 7, when the incident light is circularly polarized light, there is no NLS signal for 1 mm thick toluene; however, there is NLS signal for 2 mm thick toluene. If the polarization dependence is really the intrinsic property of molecules to polarized light, there should be no NLS signal for 2 mm thick toluene as in the 1 mm thick toluene case. Also, circularly polarized light could not cause NLS no matter how large the intensity is; however, we observed tiny NLS signal in a circularly polarized light OA Z-scan trace at higher input energy (not shown in figures). During light propagating in the sample, other optical parameters of the pulses were similar for these polarized lights except the polarization state and light intensity. So the polarization dependence should originate from intensity.

We calculate the maximum intensity at the exit face of sample against Z position when the sample is moved along the Z axis by using the following equations [12]:

$$\vec{E} = E_+ \frac{\hat{x} + i\hat{y}}{\sqrt{2}} + E_- \frac{\hat{x} - i\hat{y}}{\sqrt{2}},$$

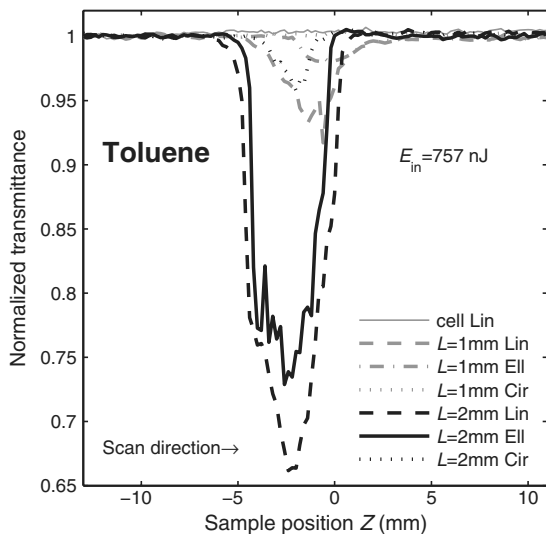


Fig. 7. Polarized light OA Z-scan traces of toluene at 757 nJ input energy for $L = 1$ mm and 2 mm.

$$\frac{1}{r} \frac{\partial}{\partial r} \left(r \frac{\partial E_{a,\pm}(r,z,t)}{\partial r} \right) - 2i\kappa \frac{\partial E_{a,\pm}(r,z,t)}{\partial z} - \kappa^2 E_{a,\pm}(r,z,t) + \epsilon_{\pm}^{\text{eff}} \kappa_0^2 E_{a,\pm}(r,z,t) = 0,$$

where \vec{E} is the electric field vector and E_+ and E_- are the left- and right-hand circular component of electric field, respectively. $\epsilon_{\pm}^{\text{eff}} = 1 + 4\pi\chi^{(1)} + 24\pi[\chi^{(3)}_{xyyx}|E_{\pm}|^2 + (\chi^{(3)}_{xyyy} + \chi^{(3)}_{xyyx})|E_{\mp}|^2]$ are the effective susceptibilities. $\kappa_{\pm} = n_{\pm,0}\kappa = n_0\omega/c$ is the wave vector of the two circular components [9,12]. In the light propagation simulation based on above equations, the self-focusing effect had been taken into account, but other nonlinear effects had not been taken into account (such as self-phase modulation and NLS, which will reduce the true intensity). We just want to present that the quantitatively self-focusing effect could cause the dependence of the maximum intensity in the sample on the polarization state of incident light; it is suitable to ignore other nonlinear effects [9]. In the simulation, the Crank–Nicolson finite-difference method was used, and the values of $\chi^{(3)}_{xyyx}$ and $\chi^{(3)}_{xyyy}$ were from Table 2.

The calculated maximum light intensity at the exit face against sample position Z for different sample length L and polarization state is shown in Fig. 8. The calculated results are qualitative because the above simulation was completed under the hypothesis of no other nonlinear effects at such large input energy. From the figure, we find that the maximum light intensity at the exit face increases with sample length L and decreases with ellipticity e although the input energy is the same. However, the occurrence of NLS and LID is greatly related to intensity [21–27]. The dependence of NLS on the polarization state and sample length could be further interpreted as follows. Once light intensity exceeds the intensity threshold of NLS (such as, the intensity indicated by the red horizontal line in Fig. 8; the selection of the intensity threshold in Fig. 8 is based on the occurrence of NLS in Fig. 7 for different polarized light), the scattering takes place [21,22]. At the same input energy and sample length, both the maximum intensity in the sample and the transverse area of intensity exceeding the NLS threshold decrease with ellipticity e . This transverse area determines the amount of liquid molecule for NLS. So the NLS signal intensity decreases with ellipticity e . For the same input energy and ellipticity, the maximum intensity in the sample increases with sample length due to self-focusing effect (as shown in Fig. 8). And the amount of liquid molecule for NLS increases with sample length. So the NLS signal intensity increases with sample length. In addition, for the same input energy, the Z position of intensity equals

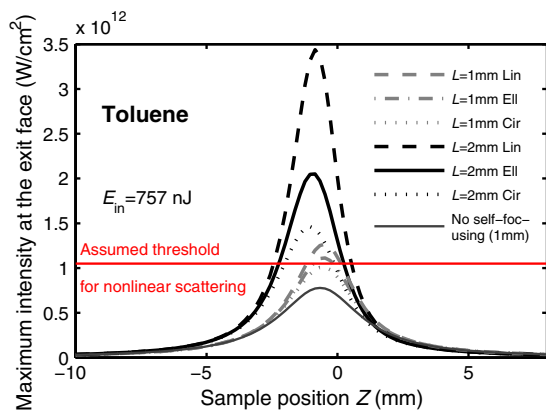


Fig. 8. (Color online) Calculated maximum intensity at the exit face of sample against position Z for different sample length and polarization state.

the intensity threshold of NLS (i.e., the Z position corresponding to the intersection of the red line and intensity curve in Fig. 8) and is getting away from the focus when the ellipticity e decreases. The Z position for observing NLS is getting away from the focus with the decrease of ellipticity e .

The dependence of NLS signal intensity on polarization in ODCB and DMF had been studied in the same way. The OA Z -scan traces with different polarized light are presented in Figs. 9 and 10 for ODCB and DMF, respectively. From these figures, we find that the NLS signal intensity of the two solvents decreases with ellipticity e as in toluene.

The OA Z -scan trace features of ODCB are quite different from those of toluene and DMF. When the sample was transferred from prefocus to focus, the normalized transmittance decreased abruptly from 1. Also, the position (Z_{decrease}) of starting to decrease was getting away from the focus as ellipticity e decreased. After the sample passing the focus, the transmittance increased while the sample was being moved away from focus. When the sample passed the position $-Z_{\text{decrease}}$, the transmittance was still smaller than 1. Also, a

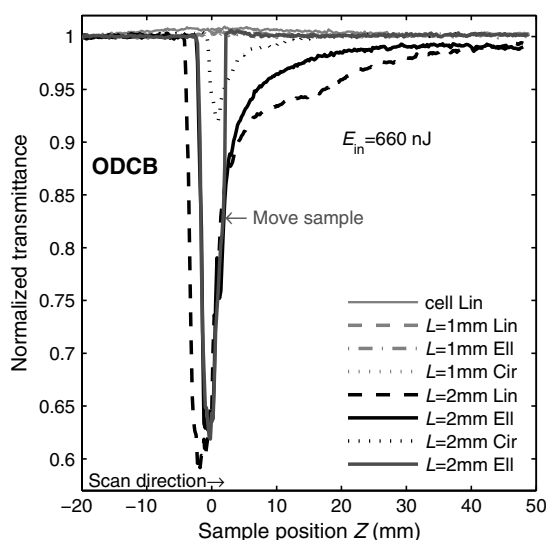


Fig. 9. Polarized light OA Z -scan traces of ODCB at 660 nJ input energy for $L = 1$ mm and 2 mm (the position of arrow marked by “Move sample” is where we laterally moved the sample at the plane perpendicular to the light axis).

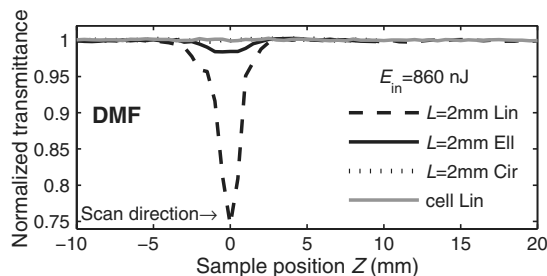


Fig. 10. Polarized light OA Z -scan traces of 2 mm thick DMF at 860 nJ input energy.

long distance was still needed for the transmittance to return to 1. These transmittance curves of ODCB are unsymmetrical respected to the focus [10]. In addition, the OA Z -scan trace feature greatly depends on scanning direction as shown in Fig. 11.

As the elliptically polarized light OA Z -scan trace of 2 mm thick ODCB shows in Fig. 9, when the sample was moved away from focus, the NLS signal existed although the scattering signal intensity was decreasing. The NLS signal could disappear immediately if we move the sample laterally (in the $x-y$ plane, which is perpendicular to the optical axis Z ; the movement operation is indicated by the “move sample” arrow in Fig. 9; the Z_{move} position for movement operation satisfied $|Z_{\text{decrease}} - Z_{\text{focus}}| < Z_{\text{move}} - Z_{\text{focus}}$). When we moved the sample laterally, we just changed sample to a fresh one, and the light intensity distribution in the sample had not been changed, but the NLS signal disappeared immediately. In other words, when the sample is placed at the postfocus position (to the focus distance is larger than $|Z_{\text{decrease}} - Z_{\text{focus}}|$), there is NLS if the light incidents into the sample that has been irradiated by larger intensity at focus; there is no NLS if the light incidents into the fresh sample. The sample irradiated by larger intensity at focus should be damaged, and the NLS signal is from the damaged sample. The scattering phenomenon from LID has been also observed in other materials [21]. Furthermore, the NLS of ODCB shown in Fig. 9 could be interpreted in the following way: once the intensity exceeds the LID threshold, the sample is damaged, and the NLS takes place. When the sample is moved from prefocus to focus, more and more sample is damaged. At the same time, some damaged sample could be replaced by a new solvent molecule due to molecule flow. However, the fresh molecule was damaged by the laser pulse near the focus, so the NLS signal was enhanced. When the sample was moved away from focus to postfocus, some damaged molecules are replaced

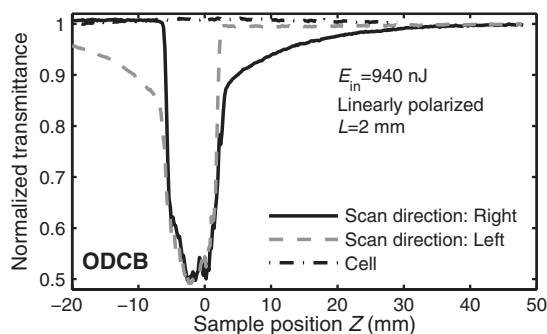


Fig. 11. OA Z -scan traces of ODCB against scanning direction.

Table 3. Viscosity of Toluene, ODCB, and DMF at $T = 25^\circ\text{C}$

	Toluene	ODCB	DMF
Viscosity (cP)	0.55 (25 °C)	1.32 (25 °C)	0.79 (25 °C)

continually by new solvent molecules. The amount of damaged solvent molecules within the light beam decreases, so the NLS signal intensity decreases. However, there was still NLS for ODCB even though the maximum intensity was smaller than the damage threshold. It is attributed to the fact that not all of the damaged molecules within light beam could be replaced by new molecules soon enough. Also, the light beam with intensity lower than the NLS threshold could be scattered by damaged molecules. If we move the sample laterally, the molecular region interacting with the light beam has been changed totally, and the NLS disappears immediately. So the OA Z -scan trace feature should be related to molecule flow rate (i.e., $1/\text{viscosity}$), and the NLS threshold is related to the LID threshold of solvent molecular.

The NLS in toluene and DMF might be accompanied with optical damage too. The LID has been observed in many dielectric materials at high light field [21–27]. If the inference that NLS is accompanied with an LID sample in these solvents is true, we could understand why the OA Z -scan trace feature is different for the three solvents. As listed in Table 3, the viscosity of ODCB is much larger than that of toluene and DMF [43]. More time is needed for the ODCB molecule to be replaced, and the OA Z -scan trace shape should be quite different for ODCB, which has been confirmed by the OA Z -scan measurements of these solvents (comparing Figs. 7, 9, and 10).

Anyway, the NLS in these solvents depends on the polarization state of incident light. Also, the dependence should originate from the polarization characteristics of the self-focusing effect, which relates to polarization characteristics of NLR. The NLS intensity in these solvents could be controlled by changing the polarization state of the incident beam.

4. CONCLUSIONS

Both NLR and NLS in the three solvents (toluene, ODCB, and DMF) are functions of the polarization state of incident light. The polarization dependences of NLR and NLS originate from the anisotropy of $\text{Re}(\chi_{xyyx}^{(3)})$ for different polarized light. In addition, the values of third-order nonlinear susceptibility tensor elements of the three solvents were determined at the fs time scale. These values could be useful in nonlinear optical parameters measurements of these novel materials dissolved in these solvents.

ACKNOWLEDGMENTS

This work was supported by the Chinese National Key Basic Research Special Fund (grant 2011CB922003), the National Natural Science Foundation of China (grants 10974103 and 11174159), and the China Postdoctoral Science Foundation funded project (grant 2012M510743).

REFERENCES

1. Yu. P. Svirko and N. I. Zheludev, *Polarization of Light in Nonlinear Optics*, Wiley-VCH (2000).

2. J. S. Aitchison, D. C. Hutchings, J. U. Kang, G. I. Stegeman, and A. Villeneuve, "The nonlinear optical properties of AlGaAs at the half band gap," *IEEE J. Quantum Electron.* **33**, 341–348 (1997).
3. D. C. Hutchings, J. S. Aitchison, B. S. Wherrett, G. T. Kennedy, and W. Sibbett, "Polarization dependence of ultrafast nonlinear refraction in an AlGaAs waveguide at the half-band gap," *Opt. Lett.* **20**, 991–993 (1995).
4. P. R. Monson and W. M. McClain, "Polarization dependence of the two-photon absorption of tumbling molecules with application to liquid 1-chloronaphthalene and benzene," *J. Chem. Phys.* **53**, 29–37 (1970).
5. M. C. Downer and A. Bivas, "Third- and fourth-order analysis of the intensities and polarization dependence of two-photon absorption lines of Gd^{3+} in LaF_3 and aqueous solution," *Phys. Rev. B* **28**, 3677–3696 (1983).
6. J. O'Dowd, W. H. Guo, M. Lynch, E. Flood, A. L. Bradley, and J. F. Donegan, "Description of polarisation dependence of two-photon absorption in silicon avalanche photodiodes," *Electron Lett.* **46**, 854–856 (2010).
7. M. Oskar van Deventer and Andre J. Boot, "Polarization properties of stimulated Brillouin scattering in single-mode fibers," *J. Lightwave Technol.* **12**, 585–590 (1994).
8. S. Odoulov, B. Sturman, L. Holtmann, and E. Kraitzig, "Nonlinear scattering in BaTiO_3 induced by two orthogonally polarized waves," *Appl. Phys. B* **52**, 317–322 (1991).
9. R. W. Boyd, *Nonlinear Optics*, 2nd ed. (Academic, 2003).
10. R. L. Sutherland, *Handbook of Nonlinear Optics* (Dekker, 1996).
11. X. Q. Yan, Z. B. Liu, X. L. Zhang, W. Y. Zhou, and J. G. Tian, "Polarization dependence of Z -scan measurement: theory and experiment," *Opt. Express* **17**, 6397–6406 (2009).
12. X. Q. Yan, Z. B. Liu, X. L. Zhang, W. P. Zang, and J. G. Tian, "Modified elliptically polarized light Z -scan method for studying third-order nonlinear susceptibility components," *Opt. Express* **18**, 10270–10281 (2010).
13. X. Q. Yan, X. L. Zhang, S. Shi, Z. B. Liu, and J. G. Tian, "Third-order nonlinear susceptibility tensor elements of CS_2 at femto-second time scale," *Opt. Express* **19**, 5559–5564 (2011).
14. S. A. Akhmanov, A. P. Sukhorukov, and R. V. Khokhlov, "Self-focusing and diffraction of light in a nonlinear medium," *Sov. Phys. Usp.* **10**, 609–636 (1968).
15. R. W. Boyd, S. G. Lukishova, and Y.-R. Shen, *Self-Focusing: Past and Present. Fundamentals and Prospects* (Springer, 2009).
16. <http://en.wikipedia.org/wiki/Self-focusing>.
17. D. Auric and A. Labadens, "On the use of a circularly polarized beam to reduce the self focusing effect in a glass rod amplifier," *Opt. Commun.* **21**, 241–242 (1977).
18. G. Fibich and B. Ilan, "Self-focusing of circularly polarized beams," *Phys. Rev. E* **67**, 036622 (2003).
19. L. A. Patel, "Effect of self-focusing on scattering of a laser beam in a collisional plasma," *J. Phys. D* **11**, 347–354 (1978).
20. B. L. Justus, A. J. Campillo, and A. L. Huston, "Thermal-defocusing/scattering optical limiter," *Opt. Lett.* **19**, 673–675 (1994).
21. H. Yu and S. Meng, "Transient stimulated Brillouin scattering and damage of optical glass," *J. Appl. Phys.* **81**, 85–88 (1997).
22. A. A. Manenkov and A. M. Prokhorov, "Laser-induced damage in solids," *Sov. Phys. Usp.* **29**, 104–122 (1986).
23. L. Sudrie, A. Couairon, M. Franco, B. Lamouroux, B. Prade, S. Tzortzakis, and A. Mysyrowicz, "Femtosecond laser-induced damage and filamentary propagation in fused silica," *Phys. Rev. Lett.* **89**, 186601 (2002).
24. B. C. Stuart, M. D. Feit, S. Herman, A. M. Rubenchik, B. W. Shore, and M. D. Perry, "Nanosecond-to-femtosecond laser-induced breakdown in dielectrics," *Phys. Rev. B* **53**, 1749–1761 (1996).
25. A.-C. Tien, S. Backus, H. Kapteyn, M. Murnane, and G. Mourou, "Short-pulse laser damage in transparent materials as a function of pulse duration," *Phys. Rev. Lett.* **82**, 3883–3886 (1999).
26. T. S. Luk, S. Xiong, W. W. Chow, X. Miao, G. Subramania, P. J. Resnick, A. J. Fischer, and J. C. Brinker, "Anomalous enhanced emission from PbS quantum dots on a photonic-crystal micro-cavity," *J. Opt. Soc. Am. B* **28**, 1365–1373 (2011).
27. C. B. Schaffer, A. Brodeur, and E. Mazur, "Laser-induced breakdown and damage in bulk transparent materials induced by tightly focused femtosecond laser pulses," *Meas. Sci. Technol.* **12**, 1784–1794 (2001).

28. D. Neher, G. I. Stegeman, F. A. Tinker, and N. Peyghambarian, "Nonlinear optical response of C_{60} and C_{70} ," *Opt. Lett.* **17**, 1491–1493 (1992).
29. Y. Liu, J. Zhou, X. Zhang, Z. Liu, X. Wan, J. Tian, T. Wang, and Y. Chen, "Synthesis, characterization and optical limiting property of covalently oligothiophene-functionalized graphene material," *Carbon* **47**, 3113–3121 (2009).
30. X. L. Zhang, X. Zhao, Z. B. Liu, Y. S. Liu, Y. S. Chen, and J. G. Tian, "Enhanced nonlinear optical properties of graphene-oligothiophene hybrid material," *Opt. Express* **17**, 23959–23964 (2009).
31. N. Venkatram, D. Narayana Rao, and M. A. Akundi, "Nonlinear absorption, scattering and optical limiting studies of CdS nanoparticles," *Opt. Express* **13**, 867–872 (2005).
32. M. Sheikh-Bahae, A. A. Said, T. Wei, D. J. Hagan, and E. W. Van Stryland, "Sensitive measurement of optical nonlinearities using a single beam," *IEEE J. Quantum Electron.* **26**, 760–769 (1990).
33. K. Y. Tseng, K. S. Wong, and G. K. L. Wong, "Femtosecond time-resolved Z-scan investigations of optical nonlinearities in ZnSe," *Opt. Lett.* **21**, 180–182 (1996).
34. T. D. Krauss and F. W. Wise, "Femtosecond measurement of nonlinear absorption and refraction in CdS, ZnSe, and ZnS," *Appl. Phys. Lett.* **65**, 1739 (1994).
35. X. Q. Yan, Z. B. Liu, S. Shi, W. Y. Zhou, and J. G. Tian, "Analysis on the origin of the ultrafast optical nonlinearity of carbon disulfide around 800 nm," *Opt. Express* **18**, 26169–26174 (2010).
36. B. Gu, J. He, W. Ji, and H. T. Wang, "Three-photon absorption saturation in ZnO and ZnS crystals," *J. Appl. Phys.* **103**, 073105 (2008).
37. S. Couris, M. Renard, O. Faucher, B. Lavorel, R. Chaux, E. Koudoumas, and X. Michaut, "An experimental investigation of the nonlinear refractive index (n_2) of carbon disulfide and toluene by spectral shearing interferometry and z-scan techniques," *Chem. Phys. Lett.* **369**, 318–324 (2003).
38. C. Kalpouzos, W. T. Lotshaw, D. McMorrow, and G. A. Kenney-Wallace, "Femtosecond laser-induced Kerr responses in liquid CS_2 ," *J. Phys. Chem.* **91**, 2028–2030 (1987).
39. Y. Sato, R. Morita, and M. Yamashita, "Study on ultrafast dynamic behaviors of different nonlinear refractive index components in CS_2 using a femtosecond interferometer," *Jpn. J. Appl. Phys.* **36**, 2109–2115 (1997).
40. D. von der Linde and H. Schüler, "Breakdown threshold and plasma formation in femtosecond laser–solid interaction," *J. Opt. Soc. Am. B* **13**, 216–222 (1996).
41. R. A. Ganeev, A. I. Rysnyanskii, and H. Kuroda, "Nonlinear optical characteristics of carbon disulfide," *Opt. Spectrosc.* **100**, 108–118 (2006).
42. D. Wang and G. Rivoire, "Large spectral bandwidth stimulated Rayleigh-wing scattering in CS_2 ," *J. Chem. Phys.* **98**, 9279–9283 (1993).
43. D. S. Viswanath, T. K. Ghosh, D. H. L. Prasad, N. V. K. Dutt, and K. Y. Rani, *Viscosity of Liquids: Theory, Estimation, Experiment, and Data* (Springer, 2007).